



Gear mesh excitation and non-uniform Rational B-Splines

A. Beinstingel^{1,2} · M. Heider¹ · B. Pinnekamp¹ · S. Marburg²

Received: 29 March 2021 / Accepted: 15 July 2021 / Published online: 15 September 2021
© Springer-Verlag GmbH Deutschland, ein Teil von Springer Nature 2021

Abstract

The noise generation of gearboxes is mainly referred to the characteristic transmission process of the mating gear teeth as the periodically changing contact conditions lead to an internal dynamic excitation. The geometry and condition of the gear teeth is therefore a significant influencing factor on the noise and vibration quality. As a result, the complex circumstances in the gear mesh require specific considerations in acoustically motivated calculations. Using Non-Uniform Rational B-Splines appears to be an appropriate alternative for numerical modeling speeding up computation time by still maintaining the underlying geometry in a highly accurate manner. The basic concept of the proposed method is explained, validated and finally applied to a sample gear with special focus on the occurring tooth root stresses during power transmission cycles.

Verzahnungsanregung und nicht-uniforme rationale B-Splines

Zusammenfassung

Die Geräuschentwicklung von Getrieben lässt sich hauptsächlich auf den charakteristischen Übertragungsvorgang der Verzahnung zurückführen, da die periodisch wechselnden Kontaktbedingungen zu einer inneren dynamischen Anregung führen. Die Geometrie und die Beschaffenheit der Verzahnung ist daher ein wesentlicher Einflussfaktor auf die Geräusch- und Schwingungsqualität. Die komplexen Verhältnisse im Zahneingriff erfordern daher eine spezielle Berücksichtigung in akustisch motivierten Berechnungen. Die Verwendung von Non-Uniform Rational B-Splines scheint eine geeignete Alternative für die numerische Modellierung zu sein, da sie die Berechnungszeit beschleunigt und gleichzeitig die zugrundeliegende Geometrie nahezu exakt beschreibt. Das Grundkonzept der vorgeschlagenen Methode wird zunächst erläutert und validiert und schließlich auf ein Beispielzahnrad angewandt. Der Schwerpunkt liegt hierbei auf den auftretenden Zahnfußspannungen während der Leistungsübertragung.

1 Introduction

The noise characteristics of gearboxes are an essential quality feature. Here, the main source of excitation is located in the gear mesh itself as the actual power transmission process leads to oscillating forces on the shafts and bearings [1, 2]. These vibrations are finally transmitted to the housing, which radiates the undesirable air-borne noise, see Fig. 1.

Primary measures for quiet operation like an improved gear geometry design are well-known. Nevertheless, designing and optimizing the acoustic quality comes along with a balancing act between noise, power density, efficiency and reliability [3]. Therefore, an efficient and accurate simulation methodology finding the most suitable geometry parameters supports the development process from the very beginning.

A numerical technique to compute the excitation behavior of the changing contact conditions during power transmission based on the Isogeometric Analysis (IGA) [4] is described in detail in [5]. This paper investigates the applicability of this simulation strategy for strength analyses focusing on the tooth root stresses occurring during power transmission. Accordingly, the numerical approach of [5] is first tested against established calculation strategies and

✉ A. Beinstingel
andreas.beinstingel@tum.de

¹ RENK GmbH, Goegginger Str. 73, 86159 Augsburg, Germany

² Germany Technical University of Munich, Chair of Vibroacoustics of Vehicles and Machines, 85748 Garching, Germany

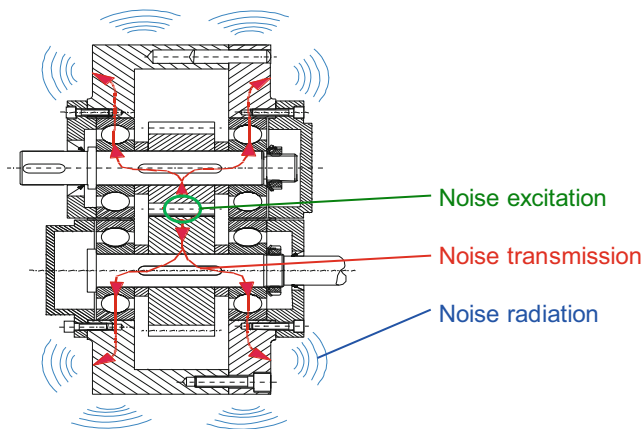


Fig. 1 Noise: Generation, transmission and radiation. *Source:* FZG TU Munich

is then applied in a dynamic simulation. Further research according to this topic can be also found in [6] and [7].

2 Gear mesh excitation and load distribution

The contact conditions of an involute gearing are periodically changing during power transmission. Besides the change in the number of involved gear teeth along the path of contact, the contact point and thus the load application point of the force to be transmitted is also shifted along the tooth profile during the meshing sequence. Hence, the variation of the acting lever arm and the tooth thickness leads to different load cases with respect to the rolling position. As a result, a single gear tooth undergoes multiple deflection states on its way from the meshing begin in point A to meshing end in point E. This total deflection mainly consists of three components [8]: tooth deflection due to bending under load, bending deflection of the gear blank or gear rim and contact deflection of surfaces under Hertzian stress.

Fig. 2 Contributions to single tooth contact deflection along the path of contact. *Source:* FZG TU Munich

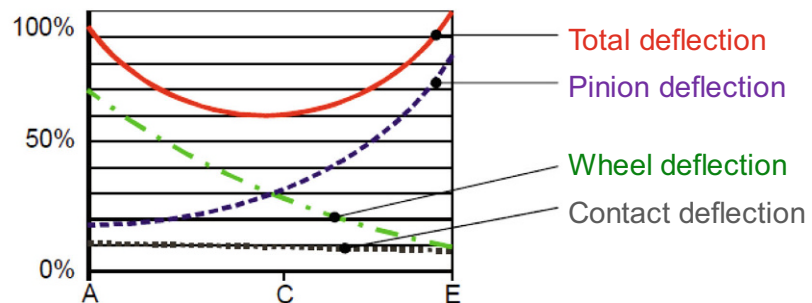
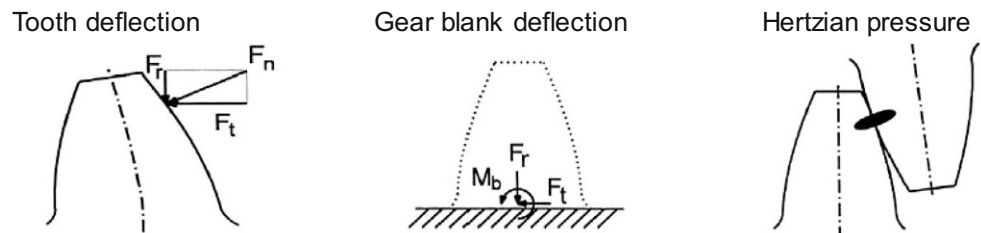
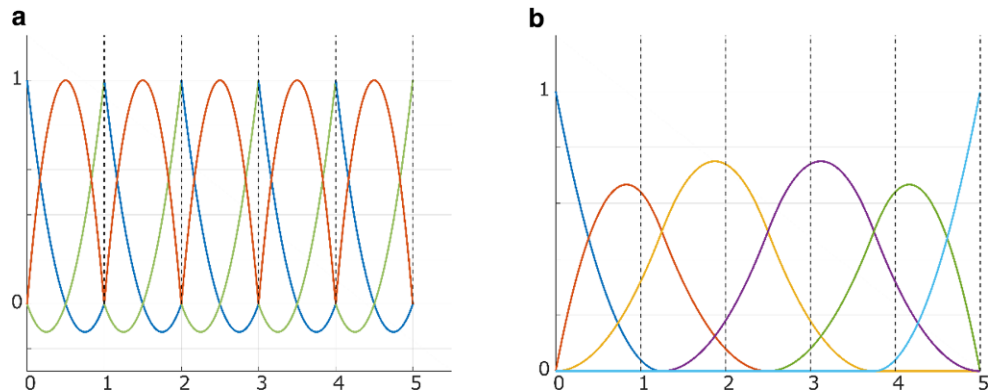


Fig. 3 Quadratic shape functions of FEM (a) and IGA (b)



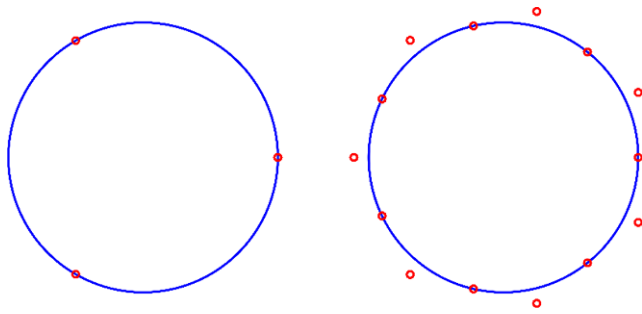


Fig. 4 Exact NURBS representation of the same circle by having a different number of control points

A schematic illustration of these deflection components is given in Fig. 2 along the path of contact.

Even with close to perfectly manufactured gear geometry, due to this elastic deformation under load, the flank position will shift against its theoretical unloaded position [9, 10]. Therefore, mesh interference between the active gear teeth with the subsequent, not yet loaded gear teeth which are about to enter the mesh is possible and hence affects again the contact conditions.

Finally, the resulting time-varying transmission error (TE) due to the deflections of all mating gear teeth is a measure of the excitation behavior of the corresponding tooth design [11, 12] and [13]. An acoustic optimization of the tooth design and hence of the contact conditions with the aim to achieve a smooth TE fluctuation consequently affects the loading conditions of all gear teeth. Therefore, an acoustic improvement can be a strength decline regarding the tooth root stresses.

Table 1 Technical data of sample spur gear

		Pinion	Wheel
Module	mm	4.5	
Pressure angle	°	20.0	
Helical angle	°	0.0	
Number of teeth	–	25	94
Tip diameter	mm	124.6	431.5
Root diameter	mm	101.2	408.2
Profile shift factor	–	0.34	–0.06
Gear width	mm	150.0	
Center distance	mm	270.0	

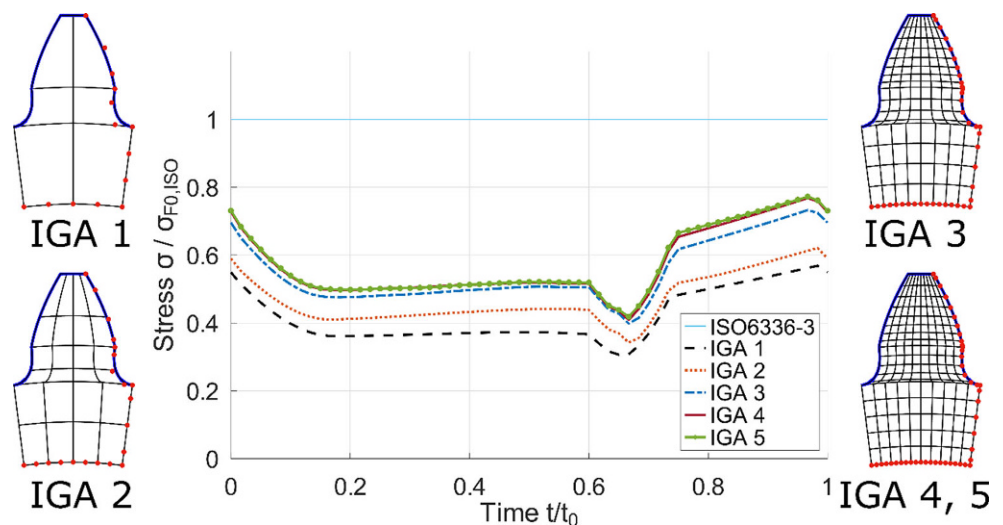
3 Non-uniform rational B-Splines

The shape of the involute gear tooth flank as well as the contour of the tooth root are complex curved geometries. Hence, the standard Finite Element Method (FEM) needs an adequately high mesh resolution to match accurately the actual tooth geometry. In contrast, the Isogeometric Analysis (IGA) is able to describe the tooth contour also with a high precision, but even with a lower number of patches (~elements), as their underlying shape functions are Non-Uniform Rational B-Splines (NURBS). This main difference between FEM and IGA is schematically illustrated in Fig. 3 by showing the corresponding shape functions with a polynomial degree of two.

In Fig. 4, the power of NURBS is demonstrated by representing a perfect shaped circle with only three control points (~nodes). An arbitrary increase of the number of control points still maintains the exact contour by simultaneously inserting additional degrees of freedom enabling the model to perform deformations that are more complex.

As a result, the IGA is an appropriate alternative for numerical modeling speeding up computation time by still

Fig. 5 Influence of mesh density on maximum tooth root stress of pinion



maintaining the underlying geometry in a highly accurate manner. The corresponding numerical meshing process of an involute gear tooth contour within the definition of the boundary conditions is explained in detail in [5] as well as the subsequent derivation of the occurring contact conditions for each rolling position, which is based on a compliance matrix approach similar to [14, 15].

4 Application

The IGA approach is applied to the sample spur gear without profile modification whose data are listed in Table 1. Here, the contact conditions—within the corresponding load distributions along the path of contact and all active tooth flanks—over one gear meshing cycle under a constant static load of 2 kNm is computed. Then, the derived load distribution serves as the basis for the computation of the tooth root stresses. As a reference quality feature, the static

stress value $\sigma_{F0,ISO}$ according to the International Standard [16] is used. Finally, the absolute maximum tooth root stress value of the IGA approach, which is found on the unloaded gear tooth side along the face width, serves as the basis for the following investigations.

At first, a brief convergence study on the influence of the numerical mesh density on the tooth root stresses (von-Mises) is conducted. Fig. 5 shows the variation of the number of patches inside the transverse section as well as the result of the maximum tooth root stress over one gear meshing period. The number of patches along the face width for IGA 1, IGA 2, IGA 3, IGA 4 and IGA 5 is 5, 10, 10, 20 and 30, respectively. The total computation time for pinion and wheel for these convergence examples is 15 s, 85 s, 235 s, 0.3 h and 0.5 h, respectively.

The result of the convergence study demonstrates again the power of the IGA approach. Even the coarse mesh IGA 1 is able to basically compute all contact conditions in a correct manner within the corresponding load distribution over one gear meshing period since all curvatures in Fig. 5 show a similar behavior. Nevertheless, the amount of the maximum tooth root stress is not sufficient for IGA 1. However, IGA 3 seems to be the best fit between accuracy and computation time.

Therefore, the numerical mesh discretization IGA 3 is taken to compare the results of the maximum tooth root stress (von-Mises and Principal) against established calculation strategies. In detail, the FVA research software packages RIKOR [17] and STIRAK [18] as well as the commercial FEM-Solver Optistruct are used to perform nonlinear static contact analysis over one gear meshing period. While the software package RIKOR calculates the stresses on an analytical basis, the software package STIRAK relies also on FEM. Fig. 6 shows a good agreement of the principal stress distribution inside the pinion tooth between the approaches IGA 3 and Optistruct at the rolling position

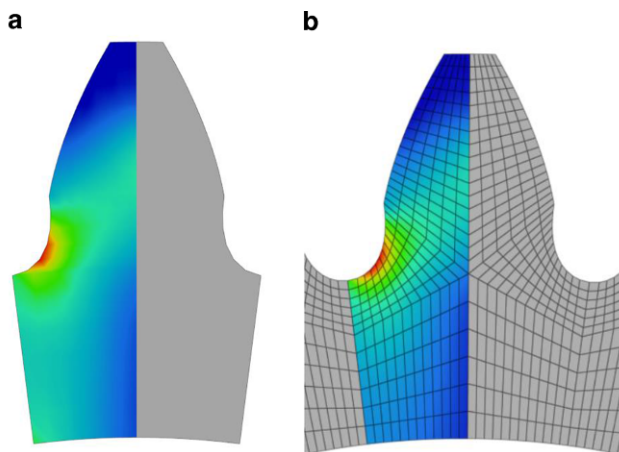


Fig. 6 Principal stress distribution of pinion at $t/t_0=0.9$; IGA (a) and FEM (b)

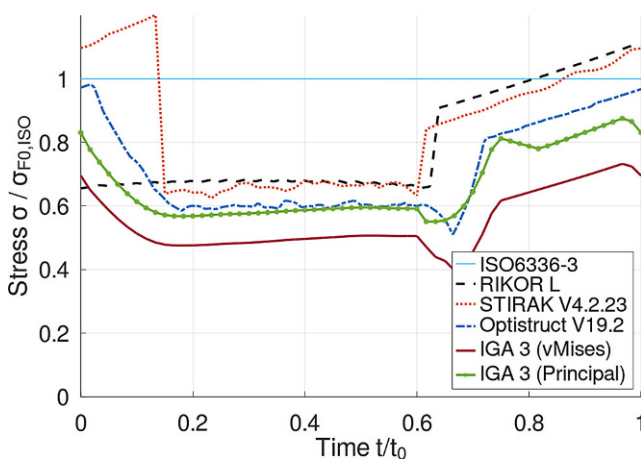


Fig. 7 Maximum tooth root stress of pinion

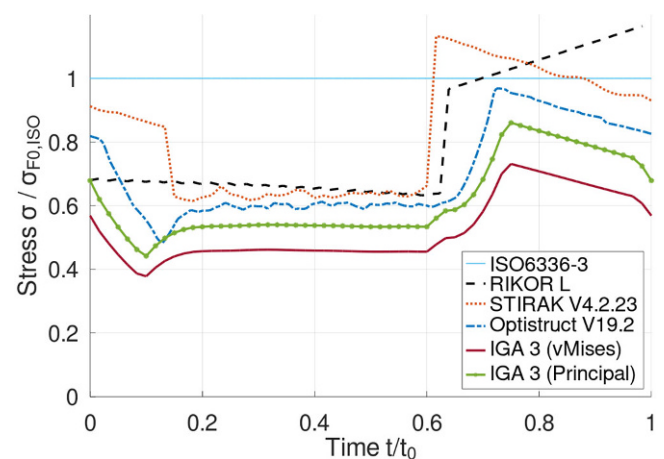


Fig. 8 Maximum tooth root stress of wheel

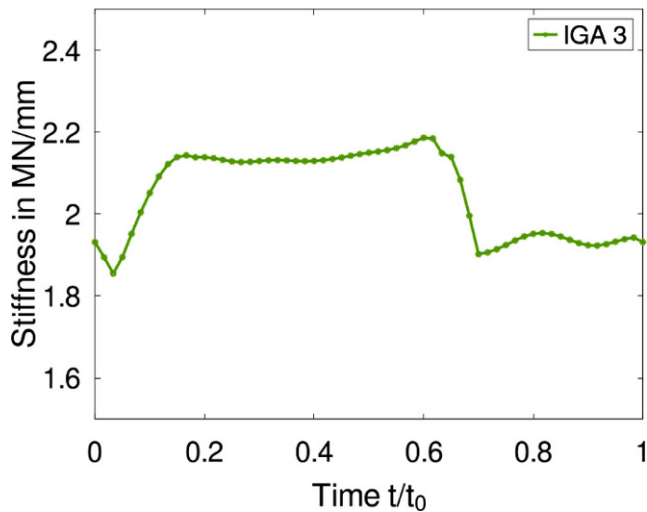


Fig. 9 Time varying gear mesh stiffness for one meshing cycle considering tip relief

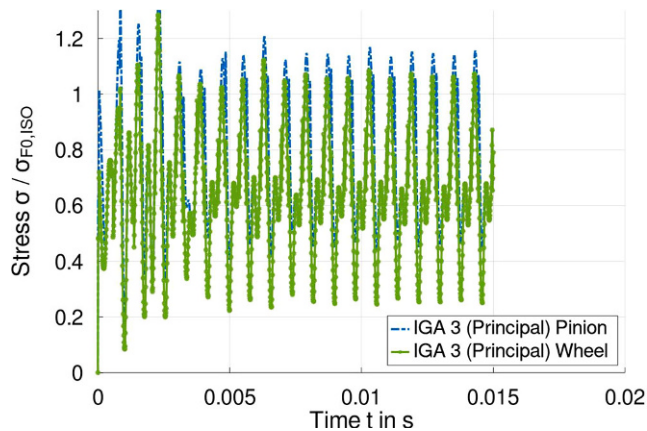


Fig. 10 Dynamic stress computed by torsional vibration model

$t/t_0 = 0.9$. All results for pinion and wheel are compared in Fig. 7 and 8.

All calculation approaches are basically in a good agreement. As expected, the principal stress of IGA 3 is higher and hence more conservative compared to the von-Mises stress of IGA 3. The software package RIKOR is a little too conservative in total as the underlying analytical computation strategy does not cover the exact shape of the tooth root contour and instead uses an approximation similar to [8]. The approaches IGA 3 and STIRAK deliver similar results outside the transition areas between double and single contact zones. This is due to the fact, that the optional consideration of possible gear mesh interference is turned off in these investigations for STIRAK. The FEM results gained by Optistruct are again very similar to the present procedure IGA 3, except that the contact is not perfectly determined in the transition areas due to the mesh quality. At this point it is noteworthy that the nonlinear FEM simulation, with almost 2 million degrees of freedom and 250

internal contact iteration steps, took about 20h of computation time on a computer with 64 cores @ 2.9/4.2GHz and 256RAM in parallel mode (MPI: 16×4).

Finally, a torsional vibration model of the sample spur gear (data in Table 1) is established with two degrees of freedom to investigate the basic dynamic behavior of the tooth root stresses of pinion and wheel. The two mating gear bodies are connected and hence excited by their corresponding time-varying gear mesh stiffness, which is determined in a preceding step under constant static load as it is explained in [5]. The fluctuating gear mesh stiffness stays linear during the complete steady-state transient simulation run as illustrated in Fig. 9.

Additionally, a damping ratio of 5% is implemented between pinion and wheel in agreement with [19]. The wheel body rotates with a constant subcritical speed at 3000rpm while having a distance of 15% to the upcoming resonance. The constant and static driving moment of the preceding investigations is applied accordingly at the pinion. The transient results of the maximum tooth root principal stress corresponding to IGA 3 for pinion and wheel are given in Fig. 10 for 19 gear meshing cycles.

The dynamic values of the maximum tooth root stresses consequently exceed the static values of the preceding investigations in an appropriate and meaningful manner. Therefore, the presented static and dynamic simulations confirm that the proposed method in [5] is also capable for the determination of static and dynamic tooth root stresses. Therefore, a subsequent and appropriate dynamic strength analysis aside the optimization process of acoustically demanded tooth designs is easily possible.

5 Conclusions

The application of Non-uniform Rational B-Splines (NURBS) for the description of the complex tooth geometry in the sense of Isogeometric Analysis (IGA) appears to be efficient for dynamic and acoustic motivated simulations. The exact tooth contour is maintained highly accurate with this special numerical meshing process by still having reasonable computation times. An appropriate adjustment of the number of patches makes the values of the tooth root stresses converge quickly. Even this additional numerical extraction of the dynamic tooth root stresses for pinion and wheel increases the computation time not significantly in transient solution runs. Therefore, it can be stated that the application of the Isogeometric Analysis supports an easy and precise dynamic strength analysis aside acoustic design reviews.

References

1. Müller R (1991) Vibration and noise excitation with toothed gears. Dissertation. Technical University, Munich
2. Heider M (2012) Schwingungsverhalten von Zahnradgetrieben. Dissertation. Technical University, Munich
3. Hoppe F, Pinnekamp B (2014) Challenge and success based on optimized gear geometries. AGMA Fall Technical Meeting
4. Cottrell JA, Hughes TJ, Bazilevs Y (2009) Isogeometric Analysis: toward integration of CAD and FEA. John Wiley & Sons,
5. Beinstingel A, Keller M, Heider M, Pinnekamp B, Marburg S (2021) A hybrid analytical-numerical method based on isogeometric analysis for determination of time varying gear mesh stiffness. *Mech Mach Theory* 160. <https://doi.org/10.1016/j.mechmachtheory.2021.104291>
6. Dai X, Cooley CG, Parker RG (2016) Dynamic tooth root strains and experimental correlations in spur gear pairs. *Mech Mach Theory* 101. <https://doi.org/10.1016/j.mechmachtheory.2016.03.010>
7. Cheng Q, Yang G, Lu J (2013) An analysis of gear based on Isogeometric analysis. *Vibroengineering PROCEDIA*, 2.
8. Weber C, Banaschek K (1953) Formänderung und Profilrücknahme bei gerad- und schrägverzahnten Rädern. *Schriftenreihe Antriebstechnik*, vol 11, pp 1–88
9. Baethge J (1969) Drehwegfehler, Zahnfederhärte und Geräusch bei Stirnrädern. Dissertation. TH Munich, Munich
10. Thoma FA (2012) Lastübertragung im verformten System Lager-Welle-Zahnrad. Dissertation. Technical University, Munich
11. Heider M, Bihl J, Otto M, Hoehn B-R, Stahl K (2013) Vibration excitation of a planetary gear stage. *International Conference on Gears*, Munich, Garching
12. Heider M, Pinnekamp B, Beinstingel A (2019) Planetary gears: excitation modes, noise and modifications. *International Conference on Gears*, Munich, Garching
13. Pinnekamp B, Heider M, Beinstingel A (2019) Specific dynamic behavior of planetary gears. Paper presented at the AGMA 2019 Fall Technical Meeting, FTM 2019.
14. Schmidt G (1972) Berechnung der Wälzpressung schrägverzahnter Stirnräder unter Berücksichtigung der Lastverteilung. Dissertation. TUtechnical University of Munich, Munich
15. Neupert B (1983) Berechnung der Zahnkräfte, Pressungen und Spannungen von Stirn- und Kegelradgetrieben. Dissertation. RWTH, Aachen, Düsseldorf
16. ISO (2006) Calculation of load capacity of spur and helical gears, ISO 6336:2006
17. Forschungsvereinigung Antriebstechnik e. V. (2011) Ritzelkorrekturprogramm (RIKOR), Version L. Bedienungsanleitung. FVA, Frankfurt/Main
18. Forschungsvereinigung Antriebstechnik e. V. (2011) FE-Stirnradkette (STIRAK) Version 4.2.21. Bedienungsanleitung. FVA, Frankfurt/Main
19. Gerber H (1984) Innere dynamische Zusatzkräfte bei Stirnradgetrieben. Dissertation. Technical University, Munich